T.1 : Research scenario of nanostructured materials at Thin Film Laboratory

L. M. Kukreja (kukreja @ cat.ernet.in)

1. Introduction

Later part of the twentieth century witnessed a spectacular development in the way we understood science of materials. Earlier notion that to change material characteristics we needed to change its chemical composition in different modes or conditions remained no more isolated. A radically different approach emerged which converged to the finding that material characteristics could also be changed by changing the size without altering the chemical composition. However the methodology of varying the material characteristics with size was feasible only within a specific size regime, called the quantum confinement regime [1] and the variation in a specific characteristic of the material invariably affected the other characteristics of the material. The possibility of tailoring the material properties by varying the size was a revolutionary idea, which enabled the emergence of a new branch of technology called "Nanotechnology". The fundamental drive to scale the height of nanotechnology to the extent that we witness today was not only to make more compact, denser and more functional integration of devices but also because newer characteristics of the materials were discovered in the nanometer size regime [1]. These characteristics offer the possibilities to push the existing frontiers of the technology in strides. Today nanoscience and nanotechnology are some of the fastest growing branches of science and technology with wide spread ramifications into areas such as nano-electronics and sensors, semiconductor lasers, communication, solar energy, medicine, and quantum computations etc.

Realizing the importance of nanostructured materials for multitude of areas of science and technology, we initiated experimental research at Thin Film Laboratory (TFL) of RRCAT in this frontline area during 1996. One of our early goals was to be able to grow structures of nanometer size with control on shape, dimensionality, size, size dispersion etc. This was rather an intricate problem. To begin with, we developed in-house a Langmuir-Blodgett set-up [2] and used it to grow nano-crystals of cadmium sulphide (CdS). However this, being a wet physico-chemical methodology, suffered from serious limitations particularly when it came to growing nanostructured materials for device applications, which was our final objective. Thus, we needed a vacuum based growth methodology for fabricating device grade nanostructures. Although a host of vacuum based growth methodologies were being used all over the world to grow nanometer size structures of different materials under variety of conditions and with varying degrees of controls, we chose a technique that was highly amenable to the research environment and could be full-grown starting from scratch in a reasonable time. This methodology was "Pulsed Laser Deposition" or PLD for short. PLD is also an advanced application of lasers in materials science, and laser is one of the strength areas of our Centre. At the incipient stages of "nanofabrication" of structures, materials scientists were understandably apprehensive about the use of PLD for growing nanometer size structures, primarily because of the inherent limitations of this technique i.e. particulate production and large average thermal energy of the plume resulting from laser ablation of the target material [1]. However, amongst other groups, we took this as a challenge and as an interesting scientific exercise to devise and evolve ways of growing nanostructures of deterministic characteristics using PLD. We have eventually succeeded in showing that despite its innate limitations there is an optimized regime of growth parameters in which PLD can indeed be applied for fabrication of high quality nanostructures.

2. Facilities to grow and study nano-materials

At TFL, we have created comprehensive infrastructure to grow a broad range of nanostructured materials *ab initio* and to investigate their different physical and compositional properties. For the PLD of ceramic materials, one needs to make high density targets for laser ablation of the materials. Fig T.1.1 shows a hydraulic press (right) to palletize the material after grinding and calcinations, and a furnace (left) with control on temperature and ambience to sinter the pallets at our laboratory.

Fig.T.1.1: Ceramic processing and target preparation systems at Thin Film Laboratory.

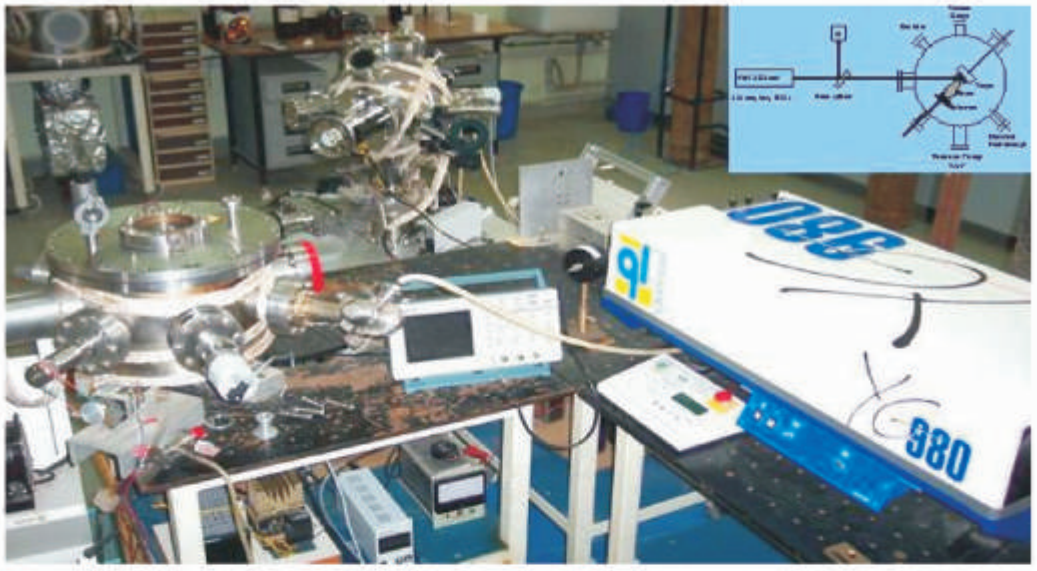

Fig. T.1.2: Pulsed Laser Deposition system. Inset shows the schematic diagram of this system.

The PLD system developed at TFL is shown in Fig.T.1.2. It consists of a commercial Q-switched Nd:YAG laser (Quantel make) capable of providing 6 ns laser pulses at a variable repetition rate up to 10 Hz, with energy per pulse up to 1.6 J in fundamental (1.06 μm), about 800 mJ in the second harmonic (533 nm), and 450 mJ in the third harmonic (355 nm). At these energies and pulse duration, practically every known material on earth can be ablated to generate its plume. However, for all practical purposes, we use the third harmonic of this laser because at the shortest wavelength, absorption of the radiation is the highest and also, the plume is particulate free. The plume thus produced is allowed to condense on a substrate, which is mounted on an electrical heater to control its temperature during the deposition of the nanostructures. Since the laser ablation results in congruent evaporation, multi-component materials can be deposited with nearly the same stoichiometry as in the target. Secondly, the rate of evaporation per pulse is so low that one can deposit a layer with control on thickness as fine as 0.1Å per pulse. At our laboratory we have two different deposition chambers, which can be first evacuated to a base pressure of 10^{-6} Torr in case of one chamber and 10^{-9} in the other one, using turbomolecular pumps and can later be filled with flowing gaseous ambient required for different deposition conditions. The gaseous ambient may be required, for example, for obtaining stoichiometric composition of the deposited structure or for supplying the species for doping purposes. Since the laser beam can pass through a gaseous ambient, PLD works as good in the presence of a gaseous ambient as in vacuum. The growth chambers are provided with a number of electrical feed-throughs for supplying electrical power to the substrate heater or for online monitoring the substrate temperature.

After deposition of the nanostructured materials, their properties of interest are studied using a variety of characterization facilities like scanning probe techniques, x-ray techniques, photoelectron spectroscopy, Raman and magnetic techniques etc., mainly at other laboratories through collaboration. At TFL, we have established the facilities to measure electrical parameters like carrier density, mobility and resistivity using van der Pauw method, and to study the photoluminescence spectroscopic properties. These facilities are shown in Fig. T.1.3.

Fig.T.1.3: Electrical characterization system (upper) and photoluminescence set-up (lower) at TFL.

3. Research areas and findings

During last one decade, nanostructures of myriad of materials, the choice of which was swayed towards the relevance to the advanced technologies being pursued at our organization, were designed, engineered and their properties were studied at TFL. The findings of our research in this field have been published in a number of papers in peer reviewed journals and in conference proceedings. A glimpse of our research findings can be obtained from the representative sub-domains, which are as follows:

3.1 Langmuir-Blodgett films of CdS nanocrystals

Cadmium sulphide (CdS) is a well known photonic material for applications in solar cells, photoconductor and nonlinear optical systems. Due to their large third-order nonlinear susceptibility, CdS nanocrystals have attracted considerable attention. We have grown oriented CdS nanocrystalline films using Langmuir-Blodgett technique [3]. Reflectivity studies on these nanocrystalline films have shown that the band-edge peak blue shifted with respect to that of the bulk CdS due to the quantum confinement effect [3].

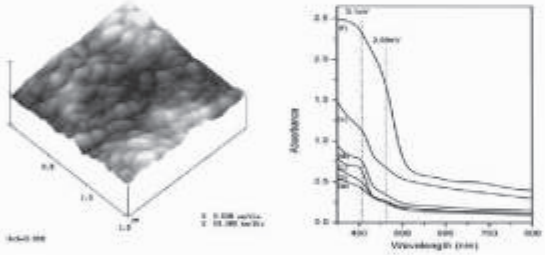

Fig.T.1.4 : AFM image of the CdS nanocrystalline film (left) and its optical absorption spectra (right) for different growth durations: (a) 1.5 h, (b) 2 h, (c) 4 h, (d) 5 h, (e) 7 h, and (f) 24 h.

We have also devised a scheme in which a combination of Langmuir-Blodgett (LB) and chemical bath techniques was used to grow oriented hexagonal CdS nanocrystalline film with thickness up to 1μm [4]. Fig.T.1.4 (left) shows the atomic force micrograph (AFM) of the film, which revealed that the crystallites were disc shaped. Right side of this figure shows the optical absorption spectra at room temperature with different growth durations of the film. All the films showed a broad exciton absorption band. This large width was attributed to a large dispersion of particle size in the film. The exciton energy was determined to be about 2.7 eV from the second derivative of these absorption spectra, which were found to be blue shifted with respect to the bulk band gap of about 2.5 eV. On the basis of this blue shift, the average particle size in these films was estimated to be about 5 nm using the effective mass approximation and including the coulomb interaction term [4]. It is interesting to note that in Fig.T.1.4 (right) we see practically no shift of the absorption peaks with the deposition time. This suggests that the average particle size remained constant with growth duration and hence it was independent of the film thickness.

3.2 Clusters in ablation plumes

Cluster physics is an important ramification of nanoscience. One of the mechanisms of the formation of clusters is the gas phase condensation and this occurs in the laser ablated plumes of the target materials also. We have studied the clusters formation in nitrogen laser (wavelength: 337nm, pulse width: 3ns) driven ablation plumes from ZnSe and ZnO targets at different fluences using a time-of-flight mass spectrometer [5]. The mass spectra of clusters are shown in Fig.T.1.5. In case of ZnSe, abundant clusters of Se and ZnSe were observed with fluence dependent distributions. At laser fluence of 1200 J-m^{-2}, besides various Zn or Se rich ZnSe clusters, magic peaks were observed at ZnSe cluster sizes of 6, 13, 19, 23 and 33 molecular numbers [5]. In case of ZnO, we detected the presence of clusters of ZnOn type, as well as a series of $(Z_nO)_n$, (Zn_nO_{n-1}) and (Zn_nO_{n+1}) type with fluence dependent distribution. Unlike in the case of ZnSe, no magic peaks were observed for ZnO. Besides the significance for understanding the fundamental

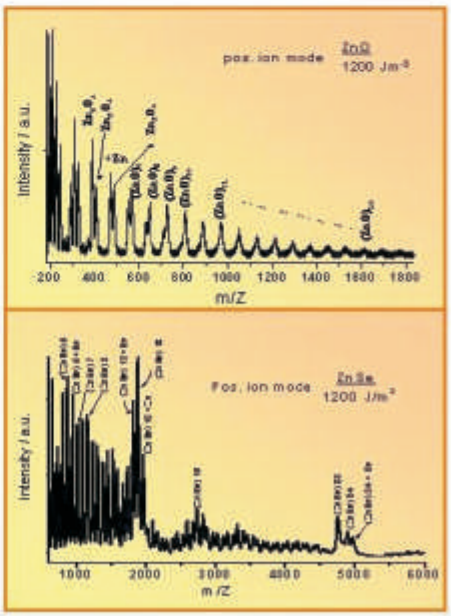

Fig.T.1.5: Time-of-flight mass spectra of ZnO (upper) and ZnSe (lower) ablation plumes with a host of clusters.

nature of the cluster formation, these studies have important implications for the PLD of nanostructures. The laser fluence at which formation of stable clusters (magic peaks) initiates should be excluded for PLD.

3.3 ZnO quantum dots

Currently ZnO, with its direct band gap of about 3.3 eV at room temperature, is a semiconductor of immense interest for blue and ultra-violet (UV) photonic devices. The large exciton binding energy of ~ 60 meV allows the excitonic transitions at room temperature in ZnO. Besides this, it is a well-known rugged and radiation hard material for oxygen gas sensors, surface acoustic wave devices, varistors, resonant tunneling devices, transparent conductors, UV screens etc. The evolution of next generation photonic devices and sensors necessitates research on quantum structures of ZnO. Research on quantum dots (QDs) of ZnO is particularly interesting for the development of nano-regime sensors, photonic devices, catalytic and other chemical systems (for example ZnO QDs are known to remove arsenic from water). We have grown multilayer of ZnO quantum dots of varying size embedded in alumina matrix on sapphire substrates by PLD and investigated

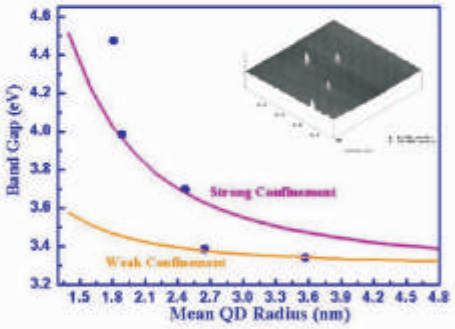

Fig.T.1.6: Experimental (filled circles) and theoretical (continuous curves) dependence of band-gap of the ZnO QDs on their mean radius. Inset shows the AFM of the QDs.

their structural and optical properties [6, 7]. Fig.T.1.6 (inset) shows the atomic force micrograph of the ZnO QDs grown by PLD. From the AFM and transmission electron microscopy (TEM) [7], we calculated the mean size and size distribution of the QDs deposited at different times. From the optical absorption studies, we calculated the band-gaps of the QDs of different sizes. Fig.T.1.6 shows these experimental values of the band-gaps (filled circles) as a function of the mean QD radius. To explain these data, we proposed two confinement domains. In the size domain where the quantum dot size was smaller than the excitonic Bohr radius (calculated to be about 2.2 nm), it was plausible that the exciton may not exist and therefore holes and electrons would experience a strong confinement with a characteristic reduced mass and a coulombic interaction. Under this circumstance, the calculated values of the band-gap [7] are shown by the 'Strong Confinement' curve in Fig.T.1.6. On the other hand, when the quantum dot size was greater than the excitonic Bohr radius, the excitons can exist and therefore the coulombic interaction term was replaced by the excitonic binding energy. The calculated values of the band-gap in this case [7] are shown by the 'Weak Confinement' curve in Fig.T.1.6. The fit of the theoretical curves with the experimental values is indicative of the efficacy of our model.

3.4 ZnO quantum wells

Current spurt of research in ZnO quantum wells (QWs) and its other variants is driven by an almost visible possibility of developing ZnO based quantum well devices such as photodiodes, light emitting diodes and laser diodes. We have grown ZnO/MgZnO multiple quantum wells (MQWs) of the well layer thickness in the range of ~1 to 4 nm on sapphire substrates by PLD using an in-house developed buffer assisted growth scheme [8]. We succeeded in observing efficient room temperature photoluminescence from these MQWs, to the best of our knowledge, for the first time [9].

Fig.T.1.7 (inset) shows a schematic of the MQW structure. Ten periods of MgZnO/ZnO layers were grown with a barrier layer thickness of ~ 8 nm and well layer thickness in the range of ~ 1 to 4 nm in separate MQWs. The optical absorption spectra of these MQWs and those of ~200 nm thick films of ZnO and MgZnO taken at room temperature are shown in Fig.T.1.7. These spectra revealed an average transmission of ~80% in the visible region for all the MQWs samples. Each absorption spectrum of the

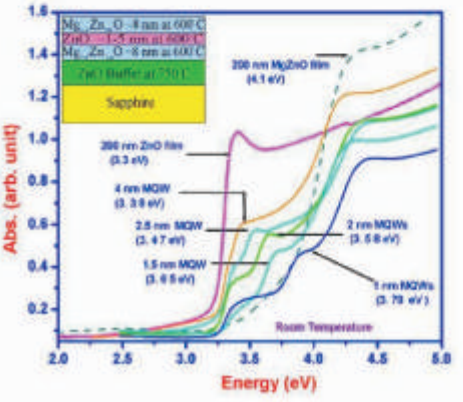

Fig.T.1.7: Schematic of the ZnO quantum well (inset) and its absorption spectra at different well layer thickness.

MQWs consists of three well resolved features. The broad shoulders at ~ 3.3 and ~4.1 eV correspond to the ZnO buffer layer and the MgZnO barrier layers respectively [9]. The central peaks in these absorption spectra are found to correspond to the n=1 excitonic transition of the ZnO quantum wells. It can be seen that this peak undergoes monotonic blue-shift with decreasing well layer thickness from 4 nm to 1 nm as expected from the quantum confinement effects [1].

The photoluminescence (PL) spectra of the MQWs, obtained with excitation from a He-Cd laser operating at 325 nm are shown in Fig.T.1.8. Along the horizontal progression of the PL peaks in this figure, it can be seen that as the well layer thickness was decreased from ~ 4 nm to 1.5 nm the PL peak shifted from ~3.36 to 3.67 eV. Along the vertical progression of the PL peaks in Fig.T.1.8, it can be observed that for a particular well layer thickness of 2.5 nm, as the temperature of the MQWs is increased, the PL peaks not only broadened but they also showed a monotonic red shift [9]. The PL peaks from ZnO MQWs of well layer thickness shorter than 2 nm at 10 K obtained by using an ArF excimer laser operating at 193 nm as excitation source are shown in the inset of Fig.T.1.8. The spectral positions of all the PL peaks are theoretically found to be in conformity with the size dependent quantum confinement effect [9]. Armed with this growth methodology and the band-gap studies, one can deploy these ZnO MQWs for a host of device and research applications.

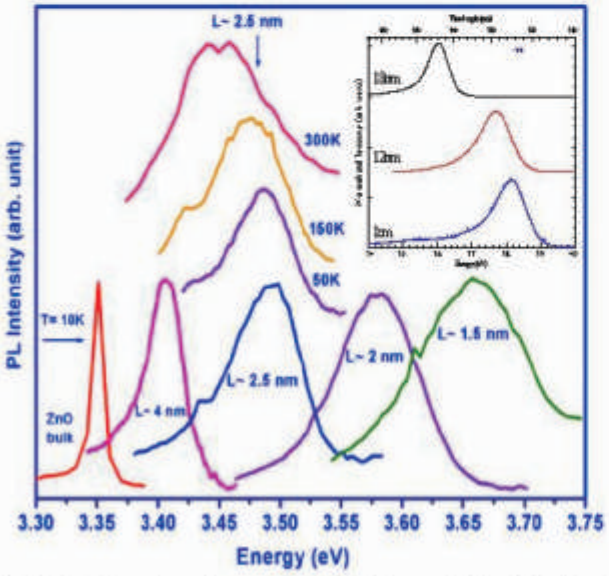

Fig.T.1.8: Photoluminescence (PL) from ZnO MQWs of different well layer thickness (L) and at different temperatures. Inset shows PL from the MQWs of different L at 10 K using ArF excimer laser as excitation source.

3.5 Silicon quantum dots

As we all know, silicon (Si) is the mainstay material of the contemporary electronic industry. But due to its indirect band-gap, which under normal circumstances prevents light emission, applications of Si in photonic devices are restricted. However the observation of strong luminescence in UV-visible spectral range and recent observation of optical gain from Si nanoparticles make them a promising option for photonic applications. Consequently currently there is worldwide interest in growing Si nanoparticles and studying their characteristics. We have grown Si nanoparticles using a novel in-house developed methodology of off-axis PLD [10], schematically shown in Fig.T.1.9(a). This methodology was found to be very effective in preventing the deposition of micron size chunks as observed in normal PLD [10]. The resulting chunk free Si nanoparticles are shown in the TEM of Fig.T.1.9 (b).

Optical transmission spectra of the Si nanoparticles of different sizes, recorded at room temperature, shown in Fig.T.1.9 (c), revealed that their band edge shifted to the lower wavelength region with decreasing size of these particles [10]. Albeit these Si nanoparticles had large size dispersion, we are currently evolving schemes to grow nanoparticles with extremely narrow size dispersion. Efforts are also underway to grow Si nanoparticles embedded in SiO_2 or other suitable host materials for optical gain media.

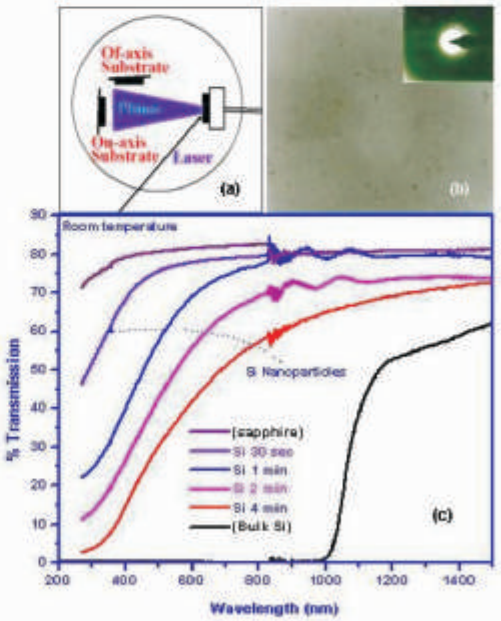

Fig.T.1.9: Schematic of the off-axis PLD (a), dark field TEM of the resulting Si nanoparticles with the selective area diffraction pattern (b) and their transmission spectra (c).

3.6 Ultra-thin high-k dielectric oxide films

Downscaling of device dimensions is a pressing problem for the development of new generation MOS technology. Due to incessant efforts of downscaling, the thickness of SiO_2 gate dielectric has already reduced to a few monolayers. Further thinning of SiO_2 poses several challenges, including control of growth and uniformity of ultra-thin SiO_2 dielectric films. Currently, the semiconductor industry is using conventional SiO_2 growth techniques such as rapid thermal oxidation. We have devised a more controlled and cleaner technique to grow ultra-thin SiO_2 films using a pulsed laser [11]. In this technique the nanosecond laser pulses are used to heat the silicon wafer surface in O_2 ambient [11]. The resulting SiO_2 films show improved dielectric characteristics which are suitable for applications in ULSI technology [11].

We have recently extended the laser oxidation scheme further to a DC discharge assisted laser oxy-nitridation scheme of silicon because nitridation is known to improve the dielectric characteristics of SiO_2. In this case the Si substrates were heated by using the 3rd harmonic of the Nd:YAG laser in the presence of DC discharge in nitrogen and oxygen ambient in the growth chamber. Schematic of the growth setup is shown in Fig.T.1.10 (left). The x-ray photo-electron spectrum confirmed the presence of oxygen and nitrogen in the grown over layers and hence the formation of silicon oxy-nitride.

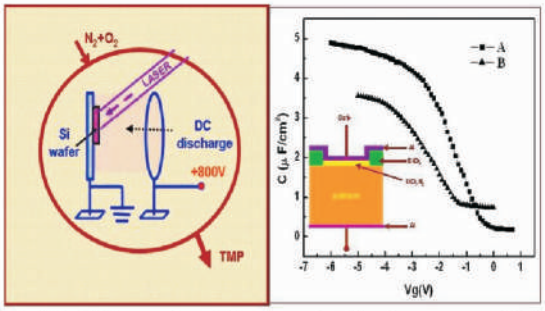

Fig.T.1.10: Schematic of the oxy-nitridation set-up (left) and the C-V characteristics (right) with N:O::1:1 (A) and 1:3 (B) of the dielectric layers in a MOS capacitor (inset right).

Studies on the MOS capacitors with dielectric layer grown through such an oxy-nitridation process revealed improved characteristics than those without nitridation. The Capacitance-Voltage measurements, shown in Fig.T.1.10 (right) on the capacitor structures, shown schematically in the inset on right, with silicon oxy-nitride as gate dielectric revealed an effective dielectric thickness in sub-nanometer range, perhaps for the first time. Further investigations on this high-k dielectric material are underway.

3.7 Nanostructured field emission materials

The phenomenon of field emission [12] is well known to have diverse technological applications in flat panel displays, microwave generation, and vacuum micro/nano-electronic devices. Currently there is a growing interest in the development of field emission cathodes using anisotropic nanostructured materials primarily because it is easier to generate nearly mono-energetic electron beam by accurately controlling the density and geometry of such field emitters. These emitters inherently fulfill the objective of obtaining higher emission current density at lower onset voltage, compared to the conventional cold cathodes. We have lately carried out research on nanostructured field emitters of LaB_6 [12], InN [13], GaN, ZnO and a host of other materials.

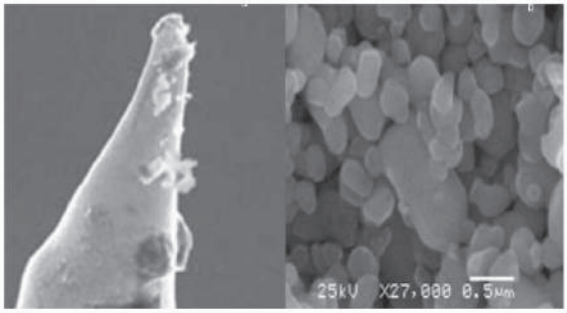

Fig.T.1.11: SEM images of as-deposited LaB_6 / W tip (a) and detailed microstructure (b).

We developed a PLD based methodology to grow coatings with nano-protrusions of LaB_6 on tungsten tip and studied their field emission characteristics [12]. Fig.T.1.11 shows the micrographs of the tip with the coating. The field emission was shown to be originating from the nano-protrusions on the LaB_6 surface [12]. We have also deposited InN thin films on c-axis oriented Al_2O_3 substrates using the DC plasma assisted pulsed laser deposition technique to study its field emission characteristics [13]. The surface morphology of these films, as investigated by AFM, consisted of densely packed nano-crystalline grains of InN. The Fowler-Nordheim (FN) plot was found to be linear in accordance with the quantum mechanical tunneling phenomenon [13]. To the best of our knowledge this is the first report on the study of field emission from nano-crystalline InN.

3.8 Sub-monolayer of Gold on Sapphire

Recently we carried out deposition of nano-islands of gold on (0001) sapphire substrates using PLD [14]. Nanometer size gold depositions on oxide substrates have

recently come under scrutiny since the experimental observation of their large catalytic activity. Using high resolution AFM, we observed the slow morphological dynamics of the apparently sessile gold nano-islands in normal ambient conditions [14]. The average thickness of these nano-islands was estimated to be about 0.55 Å, i.e. equivalent to one fourth of its monolayer. A de-wetted phase of the gold nano-islands in the form of beads was observed, which is shown in Fig.T.1.12. Each bead was found to be surrounded by a concentric layer, which appeared to be due

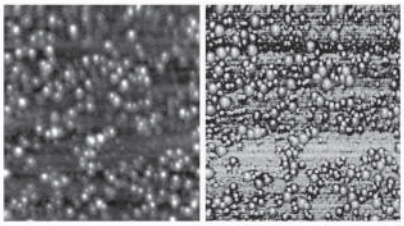

Fig.T.1.12: AFM surface topography (left) and the frequency image (right) of the de-wetted gold nano-island.

to condensed moisture from atmosphere since dehydration of the sample in vacuum with molecular sieves eliminated the corona layer completely. While the shape and size distributions of the as-prepared Au nano-islands were attributed to the specific deposition technique of PLD, the de-wetting and bead formation under ambient conditions could probably be due to the moisture or even other airborne species induced modification of the surface interactions [14]. These observations are expected to have implications for our understanding on the wetting characteristics of gold on oxide substrates in sub-monolayer regime.

4. Future plans

In near future we envisage augmenting our PLD facilities particularly by adding one high pulse energy excimer laser. This is imperative to try out ideas about different schemes of growing nanoparticles such as those of Si and ZnO with narrow size dispersion. We also intend to establish an Atomic Layer Deposition system for growing oxide semiconductors and their near relatives with determinism and control of atomic scale precision. On materials and purposes aspects, we plan to further the ongoing research on laser and discharge induced oxy-nitridation of silicon to develop improved high-k dielectric films for sub-nanometer regime MOS technology, extend our domain of expertise on ZnO nanostructures to its potential applications for field emission systems and low dimensional electron systems, continue research on Si nanoparticles for their possible application as an optical gain medium and initiate work on nanostructures of diluted magnetic semiconductors to study their opto-magnetic characteristics.

For updates about our research, please visit the website:- http : // www.cat.gov.in / technology / laser / lmddd / tfl / index.html.

Acknowledgements.

The outline of our research and development activities recounted in this article is due to the team work carried out with my colleagues at TFL and collaborators from our Centre, Indian Institute of Technology Madras, Pune University, Tata Institute of Fundamental Research, UGC-DAE Centre for Scientific Research, and Universities of Muenster and Ulm, Germany.

References

1. L. M. Kukreja, B. N. Singh and P. Misra, *Invited review* in BOTTOM-UP NANOFABRICATION, K. Ariga and H. S. Nalwa (Eds.), American Scientific, California (2007), *In press*
2. C. P. Navathe, B. L. Dashora, U. N. Roy, R. Singh, S. Maheshwari and L. M. Kukreja, *Meas. Sci. Technol. 9,* 540 (1998).
3. U. N. Roy, K. Mallik and L. M. Kukreja, *Appl. Phys.* A 67, 259 (1998).
4. U. N. Roy and L. M. Kukreja, *J. Crys. Growth* 250, 405 (2003).
5. L. M. Kukreja, A. Rohlfing, P. Misra, F. Hillenkamp and K. Dreisewerd, *Appl. Phys.* A 78, 641 (2004).
6. L. M. Kukreja, S. Barik and P. Misra, *J. Crys. Growth* 268, 531 (2004).
7. S. Barik, A. K. Srivastava, P. Misra, R. V. Nandedkar and L. M. Kukreja, *Solid State Communications,* 127, 463 (2003).
8. P. Misra and L.M. Kukreja, *Thin Solid Films* 485, 42 (2005).
9. P. Misra, T. K. Sharma, S. Porwal and L. M. Kukreja, *Appl. Phys. Lett.* 89, 161912: 1 - 3 (2006).
10. J. R. Rani, S. Barik, P. Misra, T. A. Khan, A. K. Srivastava, C. M. Negi, R. V. Nandedkar, N. DasGupta, V. P. M. Pillai, P. K. Sen and L. M. Kukreja, *Physics of Semiconductor Devices* vol. 2, K. N. Bhat and A. DasGupta (Eds.), Narosa Publishing House, New Delhi, 1047 (2004).
11. R. Singh, R. Paily, A. DasGupta, N.DasGupta, P.Misra and L. M. Kukreja, *Electronics Letters,* 40 (25), 1 (2004).
12. D. J. Late, M. A. More, D. S. Joag, P. Misra, B. N. Singh and L. M. Kukreja, *Appl. Phys. Lett.,* 89, 123510: 1 - 3 (2006).
13. K. P. Adhi, S. Harchirkar, S. M. Jejurikar, P. M. Koinkar, M. A. More, D. S. Joag and L. M. Kukreja, *Solid State Communications* 142, 110 (2007).
14. L. M. Kukreja, B. Koslowski, R. Steiner, A. Plettl and P. Ziemann, IUMRS - Intl. Conf. Advanced Materials, IISc, Bangalore, October 8-13 (2007).